



43rd European Rotorcraft Forum
Milan, Italy, 12-15 September, 2017
Paper 512

HELICOPTER WAKE ENCOUNTERS IN THE CONTEXT OF RECAT-EU

A. Jimenez-Garcia, G.N. Barakos

CFD Laboratory, School of Engineering, James Watt South Building, Glasgow G12 8QQ, U.K.

V. Treve, F. Rooseleer, V. Cappellazzo and R. Graham

EUROCONTROL Headquarters, 96 Rue de la Fusée, B-1130 Brussels, Belgium

Abstract

This work presents a first attempt to apply the RECAT-EU (European Wake Turbulence Categorisation and Separation Minima) methodology of fixed-wing aircraft separation to helicopters. The approach is based on a classification of helicopters in categories using their rotor diameter and weight combined with wake comparisons between different classes of fixed-wing aircraft and helicopters. Where necessary the upset caused by a wake encounter to a simple helicopter model is used to establish safe separation distances. The work is based on a very limited amount of data for wake strengths but shows that the principles of the RECAT-EU methodology are directly applicable to helicopters at least for landing and take-off. This research calls for further measurements of helicopter wakes with modern methods so that the suggested separation distances can be further ascertained and ultimately refined allowing for better and safer integration of fixed and rotary-wing traffic at airports.

1 INTRODUCTION

Today, there are clear separation criteria between fixed-wing aircraft [1, 2, 3]. However, for encounters between helicopter wakes and fixed-wing aircraft (FWA), separation criteria are not fully established, though some guidance exists for helicopter wake encounters. For example, a three-rotor-diameter separation distance is suggested in the CAP 493, Manual of Traffic Services [1]. In addition, accidents due to wake encounters have been reported in the U.K. [4, 5], including cases where light aircraft were hit by helicopter wakes. The helicopter wake structure near the rotor is different to that of fixed-wing aircraft (see Figure 1 (a)) but further downstream it consists of a classic pair of vortices like a fixed-wing wake (see Figure 1 (b)). The properties of the wake vortices depend on the type of helicopter (weight, size, and configuration) and its operating conditions (altitude, speed, etc.). Helicopter wake encounters mostly occur around airports where helicopters are in hover or hover taxiing and other aircraft is either landing or departing. When a

helicopter is flying a low altitude, the ground effect can distort its wake vortices, while the low forward speed results in wake skew angle. All these features are perhaps more complex to what is captured by the available helicopter fly-by LIDAR-measured wake data [6, 7], where the helicopters used were flying at altitude and at high forward speed. For the landing aircraft, due to its proximity to ground, even small wake upsets could be hazardous. Flight probe tests and fly-by measurement data for a landing aircraft encountering a helicopter wake are rare, and these tests are very difficult to conduct [8].

This work presents the separation minima on approach, for helicopters using the RECAT-EU (European Wake Turbulence Categorisation and Separation Minima) method [3]. First, a comparison between the conventional/industry, ICAO, and RECAT-EU criteria used for categorisation of helicopter types is presented. Then, a wake decay model for the Puma helicopter is derived from the experimental velocity profiles measured by Köpp [7] and compared with similar curves used for fixed-wing aircraft. Moreover, the pitch angle of the

helicopters is used as a criterion of the encounter severity. Finally, the separation minima applicable to fixed-wing aircraft and helicopters are provided following the RECAT-EU Wake Turbulence scheme.

2 RECAT-EU WAKE MODELLING

This section describes the European Wake Turbulence Categorisation and Separation Minima on Approach and Departure, also known as RECAT-EU. It also provides information about the wake modelling employed to characterise the wake turbulence.

In recent years, the large demand of domestic and international flights has exceeded the capacity and efficiency of some European airports. A major parameter to increase the capacity threshold of airports is the longitudinal separation minima required between two aircraft on approach and departure. The prescribed separation minima have been dictated by ICAO (International Civil Aviation Organisation), which provides a safe separation minimum. However, advances of acknowledge in wake vortex behaviour and new measured data along with the introduction of the A380 aircraft, led to review the ICAO scheme. In this regard, the European Organisation for the Safety of Air Navigation (EUROCONTROL) has re-categorised the ICAO based on the comparison of wake turbulence generation and wake resistance between aircraft. This new scheme split the ICAO categories (Heavy, Medium, and Light) into six categories, (Super-Heavy, Upper-Heavy, Lower-Heavy, Upper-Medium, Lower-Medium, and Light) and it is based on the Maximum Takeoff Weight (MTOW) and wing span of the aircraft. Different stakeholders and agencies such as the European Aviation Safety Agency (EASA), Airbus, and ICAO have supported RECAT-EU scheme through safety case reports and technical reviews.

By redefining wake turbulence categories, the separation minima proposed by ICAO (see Table 1) can be safely decreased for arrival and/or departure. Note that, where wake turbulence comparisons are not applicable, the separation minima are prescribed by the appropriate Air Traffic Service (ATS) authority based on Minimum Radar Separation (MRS) being 3 NM (or 2.5 NM under

given specific conditions).

Tables 2 and 3 show the RECAT-EU wake turbulence distance-based and time-based separation minima on approach and departure. This scheme provides a more precise categorisation of the aircraft along with a safe and more efficient separation.

For the approach and landing phases, a follower aircraft will roll due to the vortex-induced vertical velocity generated by the leader aircraft. A severity metric used to characterise the effect of a wake vortex encounter on a follower aircraft is the Rolling Moment Coefficient (RMC). This coefficient is simple to compute and is based on the geometric parameters of the leader and follower aircraft. This metric was introduced by De Visscher *et al.* [9] and was validated against results of a wake vortex encounter flight test campaign performed by Airbus.

The initial total circulation Γ_0 of the two-vortex system can be related to the aircraft weight W_l , flight speed V_l , wing span b_l and wing and horizontal tail plane loadings:

$$(1) \quad \Gamma_0 = \frac{W_l}{\rho V_l b_l s}$$

where the sub index l refers to leader aircraft and s is the spacing factor defined as the ratio between the initial lateral spacing between the vortices b_0 , and the aircraft span b_l . The RMC induced by a vortex on the follower aircraft is defined as:

$$(2) \quad \text{RMC} = \frac{\Gamma_{tot}}{V_f b_f} \left(\frac{AR}{AR + 4} F \left(\frac{b_l}{b_f} \right) \right)$$

with

$$(3) \quad F \left(\frac{b_l}{b_f} \right) = 1 - 2 \left(2\alpha \frac{b_l}{b_f} \right) \left(\sqrt{1 + \left(2\alpha \frac{b_l}{b_f} \right)^2} - \left(2\alpha \frac{b_l}{b_f} \right) \right)$$

and $\alpha=0.035$. This coefficient is dimensionless, which makes it easy to use for global comparative assessment of different aircraft.

3 A SIMPLE HELICOPTER WAKE MODEL

A key observation is that the near-ground operations in hover-taxi require high fidelity free-wake or CFD simulations to capture the flow physics of the helicopter wake. However, before hover-taxing, during approach and far from the rotor, the wakes can be seen as simple pairs

of vortices comparable in structure with the RECAT-EU wake model. In the next section, and without downplaying the importance of the hover-taxi operations or the complexity of the rotor wake, an attempt will be made to derive separation criteria using the RECAT-EU framework.

3.1 Wake models and wake decay

Helicopter wakes can be modelled and analysed with different levels of fidelity. From prescribed wakes, to free wakes, to vortex particle and vortex transport models, all the way to fully-resolved wakes using large-eddy simulation. As Figure 1 suggests, helicopter wakes vary in their topology according to the flight regime and since this study focusses on approach and take-off with the wake of the helicopter still trailed behind it, the simple model of a rotor seen as a fixed wing of circular planform is used. This model stems from Glauert's theory and at high speed of flight it agrees with the lifting line theory that is used with the RECAT-EU approach. On the other hand, due to the employed wake model, the current study cannot cover hover/taxi operations or other near ground operations. To date, most helicopter wake studies were focused on the near-rotor wake due to its strong influence on helicopter performance. Fewer studies looked at the far wake (further than 3 rotor diameters away of the helicopter). One exception is the work of Köpp [7] that concerned LIDAR measurements of helicopter wakes, and focussed on the decay of the wake behind a Puma helicopter, at speeds of around 65kts and at distances as far as 20 rotor diameters behind the aircraft. Data from this experimental study can be used to deduce a "decay-law" for the circulation of the fully rolled up pair of vortices trailed behind the rotor disk.

3.2 Classification of helicopters

The helicopter categories are defined according to MTOW for ICAO and these categories are different to the convention used by manufactures. MTOW and diameter of the main rotor are used for the RECAT-EU system. Regarding the RECAT-EU scheme, we use the diameter of the main rotor as a characteristic length instead of the

span of the aircraft. Table 4 shows the criteria used for categorisation of helicopters based on the conventional and ICAO schemes. The industry classification includes four categories (light, intermediate, medium, and heavy), while ICAO includes the same categories except for the intermediate one. The range, and upper and lower values of MTOW used for both criteria are very different. The conventional/industry scheme seems to be more suitable for the existing helicopters, where MTOW varies from the light Schweizer 300C with 930 kg to the heaviest helicopter in service with 56,000 kg (Russian Helicopters Mi-26T). The main reason why the ICAO criteria look over-scaled for the current helicopters in service is that its categorisation was originally designed for fixed-wing aircraft, with MTOW commonly between 10-100 tons.

Figures 2 (a) and 2 (b) show the RECAT-EU criteria used for categorisation of fixed-wing aircraft and helicopters, respectively. This includes six categories based on the MTOW and span/diameter of the rotor for a fixed-wing aircraft/helicopter (from "Super Heavy-CAT-A" to "Light-CAT-F"). Using this categorisation, a wide range of different sized aircraft can be covered. However, all helicopters in service, fall in "Upper Medium-CAT-D", "Lower Medium-CAT-E", and "Light-CAT-F" because all existing helicopters have MTOW lower than 100 tons.

Tables 5 and 6 show examples of helicopters assigned to conventional/industry, ICAO, and RECAT-EU categories. The ICAO criteria provide very little grading. The conventional/industry approach has the biggest number of categories and RECAT-EU is in between.

3.3 Wake decay model for helicopters

Unlike fixed-wing aircraft, few measurements of helicopter wakes are available in the literature. Köpp [7] carried out fly-by Doppler LIDAR measurements of a Sikorsky CH-53 and Puma helicopter wakes. The experiments were conducted at the Oberpfaffenhofen airport and tangential velocities of the port-side of both rotors were measured at approximately 9 seconds after their generation. The flight parameters are listed in Table 7.

Figure 3 shows the decay of the maximum tangential velocity for the Sikorsky CH-53 (ID1 and ID3) and Puma helicopters (ID5 and ID7) at forward airspeeds of 90, 70,

and 65kt (see Table 7). After the roll-up phase, where the vortex is almost of constant strength, the decay curves are very similar between the different cases with a linear-decay. This is labelled as 'deduced' in Figure 3.

Before presenting the helicopter wake vortex circulation decay, a brief introduction of the characterisation of fixed-wing aircraft wake vortex circulation decay is given. It is well known [9] that the dimensionless decay curves of aircraft wake vortices collapse on a generic curve (see Figure 4). The total circulation of the tip vortex decreases in time, from its initial value Γ_0 following a decay curve. This is function of three parameters, the Brunt-Väisälä frequency N , which accounts for the thermal stratification, the eddy-dissipation rate (EDR) ϵ , which depends on the ambient turbulence, and the wind speed V_w .

The vortex initial total circulation is represented by Γ_0 and the initial vortex spacing by b_0 . The aircraft span is represented by b , and s is the initial lateral vortex spacing, which only depends on the aerodynamic interaction between the wing and horizontal tail plane. The initial total circulation can be computed using the weight of the aircraft W , forward airspeed V , wing span b , air density ρ , and the initial lateral vortex spacing s :

$$(4) \quad \Gamma_0 = \frac{W}{\rho V s b}$$

If we assume out-of-ground effect (OGE) conditions,

the pair of vortex sinks at a velocity equals to $V_0 = \frac{\Gamma_0}{2\pi b_0}$

with a characteristic time equals $t_0 = b_0/V_0$ (time required for the pair of vortex to sink a distance b_0 a velocity V_0).

Using the values of Γ_0 and b_0 collected by EUROCONTROL [9] and used in the RECAT_EU Safety Case [3], the obtained dimensionless decay curves are compared in Figure 5 as functions of the time (left) and distance (right). Note that, a generic speed profile has been applied to compute the distance. This speed profile is depicted in Figure 6, which is characterised by three steps; deceleration until 5 NM with a forward speed of 160 knots, stabilisation at 3NM (forward speed of 135 knots), and constant speed of 135 knots until touchdown.

Figure 7 shows a comparison of the generic dimensionless decay curves of fixed-wing aircraft (solid

line) and helicopter (dashed line) wakes. The helicopter decay curve was obtained from the maximum tangential velocity profile (shown in Figure 3 as 'deduced'). A value of 0.85 for the vortex spacing factor s was considered, which is in line with the prescribed wake model of Landgrebe [10], experimental data [11], and CFD results for helicopters [12]. An example of the radial displacements of the tip vortices as a function of the vortex age (in degrees) for the full-scale S-76 rotor blade is shown in Figure 8, reaching asymptotic values suggesting a radial contraction of 0.85. Considering Figure 7, it is interesting to note the slopes of both decay curves are very similar, which supports the idea of using the decay curve for fixed-wing aircraft to characterise the wake vortex circulation decay of helicopter.

Unlike fixed-wing aircraft, there are several approaches for helicopters based on the glide angle and forward speed (see Table 8). For this study, we only consider the first approach (3 degrees) because there are no measurements at 2,000ft for decay curves of fixed-wing aircraft to be compared to.

Figure 9 shows the dimensionless decay curves as functions of the time (left) and distance (right) for helicopters covering all possible categories, from CAT-D (Mi-26T) to CAT-F (AW109). Note that for this case, a helicopter approach at glide angle of 3 degrees and forward velocity of 70 knots was considered.

4 A METRIC FOR THE WAKE SEVERITY ENCOUNTER

Within the RECAT-EU framework a rolling moment coefficient is used to support the separation criteria [9]. This is not as straight forward for helicopter and therefore a different approach was necessary. In general, the analysis of the wake encounter requires a detailed flight mechanics model of a helicopter and piloted simulator to assess the behaviour of the vehicle during the encounter. Since this work is only a first look at the problem, the following approach was taken. Looking at the ADS33 manual, and across several manoeuvres, Level 1 handling qualities tend to correspond to upsets in pitch angles of less than 10 degrees. This is also reported in the work of Padfield [13]. We will therefore estimate the

pitch angle upsets during the time of encounter and report on that value.

The pitch angle of a helicopter encountering a vortex of velocity V_T can be approximated as follows:

$$(5) \quad \theta(t) = \frac{(V_T/\Omega R)\mu\Omega\gamma}{\left(1 - \frac{1}{2}\mu^2\right)^8} t$$

Table 9 lists the physical and geometric parameters of a generic helicopter to supply the pitch angle equation. Note that the C_T is based on the MTOW of the helicopter. Moreover, the advance ratio is defined as $\mu = \sqrt{\mu_x^2 + \mu_z^2}$.

5 SEPARATION MINIMA ON APPROACH

As mentioned, the separation minima applicable to FWA and helicopter, either as leaders or followers, are provided following the RECAT-EU WT (Wake Turbulence) scheme. The three cases considered here to suggest separation minima applicable to the fixed-wing aircraft/helicopter pair are listed in Table 10.

5.1 Helicopter leader - fixed-wing aircraft follower

The first case considered here is the helicopter acting as a leader and the fixed-wing aircraft as a follower. By comparing the wake vortex generated by the aircraft and the helicopter for the same category, we can suggest safe separation minima or safety margins. Starting with a leader and follower of CAT-F, RECAT-EU considers distance-based separation minima on approach of 3NM. A comparison of the total circulation generated by the SF-34 fixed-wing aircraft (CAT-F) and the EH-101 Merlin and AW-109 helicopters (CAT-F) are depicted in Figure 10 (a). The same methodology can be applied to helicopters of CAT-E and CAT-D to estimate a safety margin. Figure 10 (b) compares the circulation for the fixed-wing aircraft B-735 corresponding to CAT-E, the CH-53K and the CH-6 Chinook helicopters of the same category. It is seen that at 4 NM, the values of circulation for the helicopters are lower than the fixed-wing aircraft, which suggests that 4 NM is a safe margin for helicopters.

A comparison between the helicopter Mi-26T and the fixed-wing aircraft B738 of CAT-D in term of circulation is shown in Figure 10 (c). The distance-based separation

minimum on approach for a helicopter of CAT-D as a leader is 5 NM, so this is in line with the separations proposed by the RECAT-EU Safety Case.

Table 11 shows the suggested separation minima for the RECAT-EU categories for a helicopter acting as a leader and fixed-wing aircraft as a follower.

5.2 Fixed-wing aircraft leader - helicopter follower

This section presents a severity metric for the effect of a wake vortex encounter generated by a fixed-wing aircraft on a follower helicopter. The proposed metric is the pitch angle computed using geometrical parameters of the helicopter and a profile velocity of the wake vortex encounter. Moreover, the proposed metric permits us to evaluate the separation minima on approach for the pair fixed-wing aircraft/helicopter. Therefore, a reduction of the wake turbulence separations compared to either ICAO or RECAT-EU criteria can be done, while maintaining the current safety level.

Three helicopters were selected to evaluate the impact of wake vortex encounter, covering CAT-F (SA 330 Puma), CAT-D (Mi-26T), and CAT-E (CH-53K). The basic physical characteristics of the SA 330 Puma can be found in [14] and are reported in Table 12. We make the following assumptions regarding the physical parameters:

- Lock number of the blade (γ) is 11
- The blade flap stiffness (K_b) is 1
- The distance from the main rotor to the CG (h) is 2m
- The advance ratio μ is 0.12

The following fixed-wing aircraft were considered for this study; A346, B744, B764, A310, B752, B738, B735, and SF34. The values of circulation can be computed using the generic dimensionless decay curve for fixed-wing aircraft at distances dictated by RECAT-EU. Therefore, the maximum tangential velocity is expressed as function of the local circulation Γ and the rotor radius of the helicopter R :

$$(6) \quad V_T = \frac{\Gamma}{4\pi R^2}$$

This equation shows that the tangential velocity is directly proportional to the circulation and therefore the

mass of the aircraft, and inversely proportional to the rotor radius of the helicopter. Once the values of tangential velocity for each pair of aircraft/helicopter are obtained, we apply the pitch angle criteria and compute its maximum value. Table 13 shows the maximum values of pitch angles in degrees and the distance in brackets, when a wake vortex generated by a fixed-wing aircraft encounters a follower helicopter. The selected distances between the fixed-wing aircraft and the helicopters are based on the RECAT-EU criteria (see Table 2).

Since none of the angles exceed the 10-degree value suggested in the ADS33 manual, it is suggested that for the RECAT-EU distances are maintained for fixed-wing aircraft leading helicopter.

5.3 Helicopter leader – helicopter follower

The effect of the wake vortex encounter generated by a helicopter on a follower helicopter is investigated here. This case stands between Cases 1 and 3 of Table 10 and can be seen as a combination of these scenarios. The methodology employed to evaluate the separation minima on approach is based on the RECAT-EU criteria [3] with the severity metric proposed for the pitch angle.

The helicopters selected as leaders are the Mi-26T, CH-53K, and EH-101, corresponding to CAT-D, CAT-E, and CAT-F, respectively. These helicopters are the heaviest of their categories (see Table 6), so it is expected to have the largest values of circulation. The followers selected for this study are the Mi-26T, CH-53K, and SA 330 Puma helicopters, with their physical characteristics reported in Table 12. Table 14 shows the maximum values of pitch angles in degrees and the distance in brackets, when a wake vortex generated by a helicopter encounters a follower helicopter. Like for case 2, the distance between the pair helicopter/helicopter was based on the RECAT-EU criteria (see Table 2). Note that all pitch angles computed with the severity metric have values lower than the threshold of 10 degrees suggested in the ADS33 manual. Table 15 summarises the suggested separations.

6 CONCLUSIONS

The RECAT-EU methodology has been applied to helicopters and was found to provide adequate separation distances for wake encounters. The approach is based on a scheme that uses the rotor diameter and the aircraft weight to fit helicopters within the 6 RECAT-EU categories. Comparing the wake strengths of rotary and fixed-wing aircraft, mixed pairs of helicopters leading or following fixed-wing aircraft as well as helicopter/helicopter pairs can be separated. Where appropriate the upset caused by a wake encounter is used to specify a safe separation distance/time. Given the assumptions of the model, for all cases the suggested separation distances of RECAT-EU were found to be also adequate for helicopters. The scheme is simple and effective but can be further improved on two fronts. One suggestion is to gather more and better helicopter wake data using techniques like LIDAR to allow for better wake decay curves to be estimated. The second suggestion is to use piloted flight simulation to replace the wake upset criterion currently used. Both suggestions are expected to strengthen confidence on the model and could also lead to further separation improvements.

7 ACKNOWLEDGEMENTS

This work is supported by EUROCONTROL under SESAR Project 6.8.1. The authors acknowledge the use of the <http://vertipedia.vtol.org>.

8 REFERENCES

- [1] CAA, "CAP 493: Manual of Air Traffic Services Part 1," 2011.
- [2] P. Wilson, C. Lepadatu, S. Barnes and S. Lang, "Technical Report to Support the Safety Case for Recategorization of ICAO Wake Turbulence Standards: Methodology for Re-Categorization of ICAO Wake Turbulence Standards," 2011.
- [3] F. Rooseleer and V. Treve, "RECAT-EU European Wake Turbulence Categorisation and Separation Minima on Approach and Departure," EUROCONTROL, 2015.
- [4] CAA, "Aircraft accident report 1/93," 1993.
- [5] P. Wilson, C. Lepadatu, S. Barnes and S. Lang, "Technical Report to Support the Safety Case for Recategorization of ICAO Wake Turbulence Standards:

An Overview of Key Aviation Accidents Sometimes Assumed to Have Been Caused by Wake Turbulence,” 2010.

[6] S. A. Teager, K. J. Biehl, L. J. Garodz, J. J. Tymczyszczym and D. C. Burnham, “Flight Test Investigation of Rotorcraft Wake Vortices in Forward Flight,” 1996.

[7] F. Kopp, “Wake vortex characteristics of military-type aircraft measured at airport Oberpfaffenhofen using the DLR Laser Doppler Anemometer,” Aerospace Science and Technology, vol. 3, pp. 191-199, 1999.

[8] N. Matayoshi, K. Asaka and Y. Okuno, “Flight Test Evaluation of a Helicopter Airborne LIDAR,” Journal of Aircraft, vol. 44, pp. 1712-1720, Sept. 2007.

[9] I. De Visscher and G. Winckelmans, “Characterization of Aircraft Wake Vortex Circulation Decay in Reasonable Worst Case Conditions,” in 54th AIAA Aerospace Sciences Meeting, San Diego, California, USA, 2016.

[10] A. J. Landgrebe, “An Analytical Method for Predicting Rotor Wake Geometry,” AHS VTOL Research, Design and Operations Meeting, pp. 20-32, February 17-19 1969.

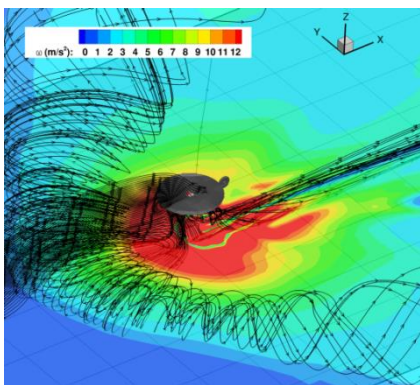
[11] A. Swanson, “Application of the shadowgraph flow visualisation technique to a full-scale helicopter rotor in hover and forward flight,” in 11th Applied Aerodynamics Conference, Monterey, California, USA, 1993.

[12] A. Jimenez and G. N. Barakos, “CFD analysis of hover performance of rotors at full-and model-scale conditions,” The Aeronautical Journal, vol. 1, no. 1231, pp. 1-39, 2016.

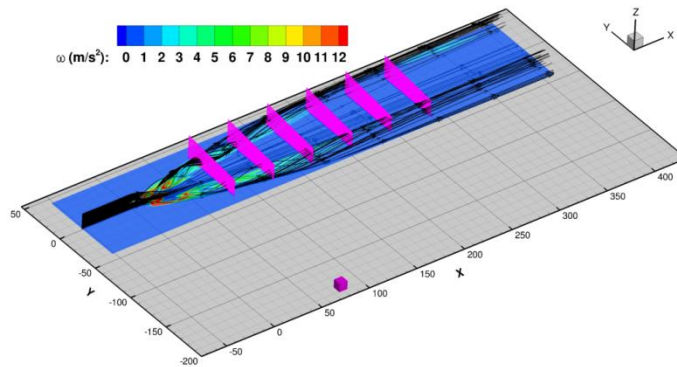
[13] B. Lawrence and G. D. Padfield, “Wake vortex encounter severity for rotorcraft in final approach,” Aerospace Science and Technology, vol. 12, pp. 385-397, 2008.

[14] G. D. Padfield, “SA 330 Puma Identification Results,” AD-A244 248, vol. 10, pp. 1-38, 1991.

9 TABLES AND FIGURES



(a)



(b)

Figure 1: (a) Near and (b) far-wakes of a light helicopter

Leader/Follower	A380-800	HEAVY	MEDIUM	LIGHT
A380-800		6 NM	7 NM	8 NM
HEAVY MTOW ≥ 136 tons		4 NM	5 NM	6 NM
MEDIUM 7 tons ≤ MTOW < 136 tons				5 NM

LIGHT MTOW < 7 tons				
------------------------	--	--	--	--

Table 1: ICAO wake turbulence categories and separation minima

RECAT-EU scheme		“SUPER HEAVY”	“UPPER HEAVY”	“LOWER HEAVY”	“UPPER MEDIUM”	“LOWER MEDIUM”	“LIGHT”
Leader / Follower		“A”	“B”	“C”	“D”	“E”	“F”
“SUPER HEAVY”	“A”	3 NM	4 NM	5 NM	5 NM	6 NM	8 NM
“UPPER HEAVY”	“B”		3 NM	4 NM	4 NM	5 NM	7 NM
“LOWER HEAVY”	“C”			3 NM	3 NM	4 NM	6 NM
“UPPER MEDIUM”	“D”						5 NM
“LOWER MEDIUM”	“E”						4 NM
“LIGHT”	“F”						3 NM

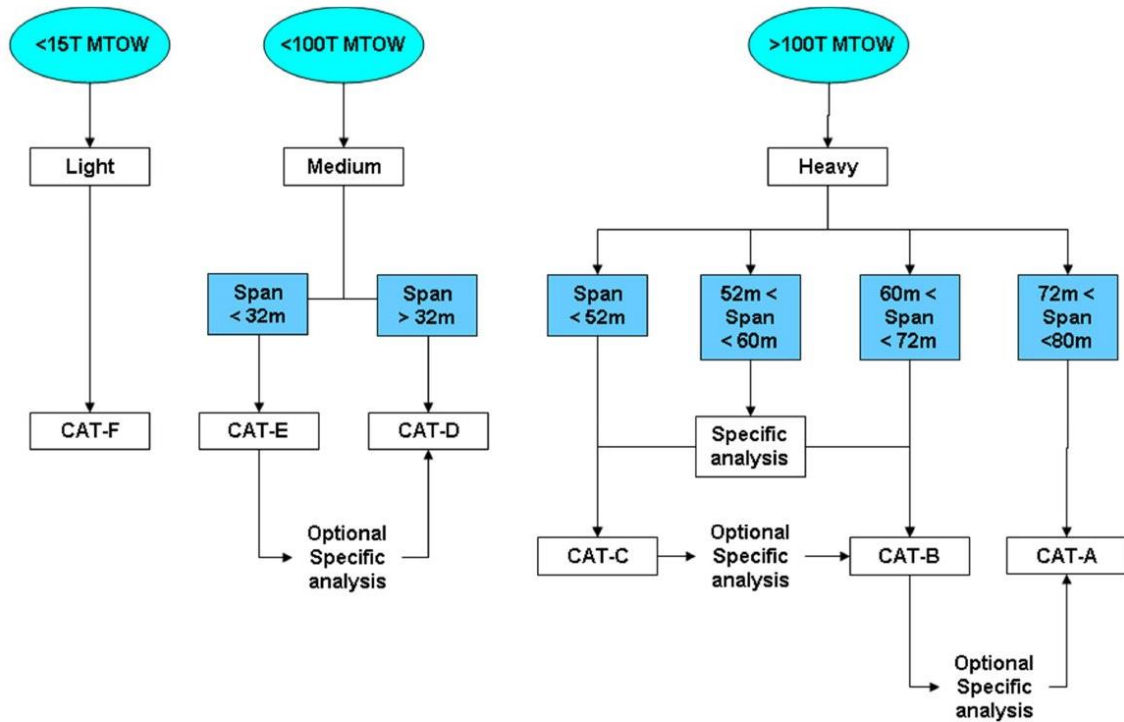
Table 2: RECAT-EU wake turbulence distance-based separation minima on approach and departure

RECAT-EU scheme		“SUPER HEAVY”	“UPPER HEAVY”	“LOWER HEAVY”	“UPPER MEDIUM”	“LOWER MEDIUM”	“LIGHT”
Leader / Follower		“A”	“B”	“C”	“D”	“E”	“F”
“SUPER HEAVY”	“A”		100 s	120 s	140 s	160 s	180 s
“UPPER HEAVY”	“B”				100 s	120 s	140 s
“LOWER HEAVY”	“C”				80 s	100 s	120 s
“UPPER MEDIUM”	“D”						120 s
“LOWER MEDIUM”	“E”						100 s
“LIGHT”	“F”						80 s

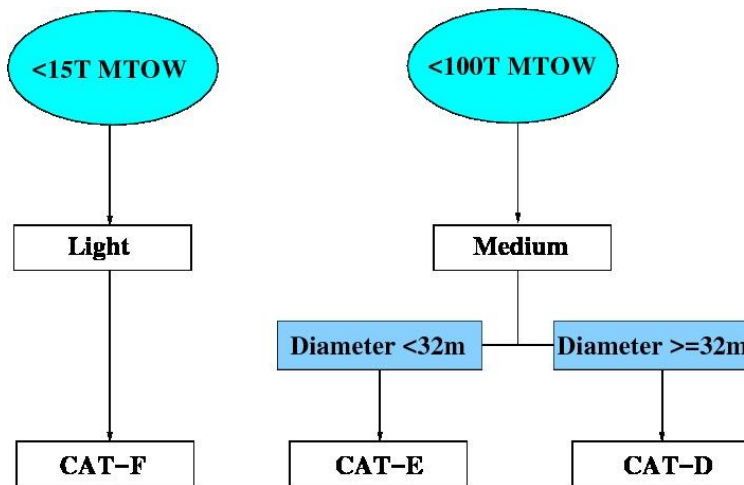
Table 3: RECAT-EU wake turbulence time-based separation minima on approach and departure

Categories	Conventional/Industry	ICAO
Light	MTOW < 1,500 kg	MTOW < 7,000 kg
Intermediate	1,500 kg ≤ MTOW < 3,000 kg	7,000 kg ≤ MTOW < 136,000 kg
Medium	3,000 kg ≤ MTOW < 6,000 kg	
Heavy	MTOW ≥ 6,000 kg	MTOW ≥ 136,000 kg

Table 4: Helicopter categorisation process based on the conventional/industry and ICAO criteria



(a) Categorisation process for fixed-wing aircraft



(b) Categorisation process for helicopter

Figure 2: Categorisation process for fixed-wing aircraft and helicopters based on the RECAT-EU criterion [3]

RECAT-EU	CAT-A	CAT-B	CAT-C	CAT-D	CAT-E	CAT-F
FWA	YES	YES	YES	YES	YES	YES
Helicopter	N/A	N/A	N/A	YES	YES	YES

Table 5: Categorisation of fixed-wing aircraft and helicopter following RECAT-EU criterion [3]

Helicopter	MTOW (kg)	Diameter 2R (m)	Conventional	ICAO	RECAT-EU
------------	-----------	-----------------	--------------	------	----------

S-300C	930	8.18	Light	Light	CAT-F
EC-130	2,427	10.69	Intermediate	Light	CAT-F
AW-109	2,850	11	Intermediate	Light	CAT-F
UH-1A	3,266	13.41	Medium	Light	CAT-F
AW-169	4,500	12.12	Medium	Light	CAT-F
EC-665	6,600	13	Heavy	Light	CAT-F
AW-139	6,800	13.8	Heavy	Light	CAT-F
SA-330	7,400	15.09	Heavy	Medium	CAT-F
UH-60A	7,622	16.36	Heavy	Medium	CAT-F
AH-64A	9,525	14.63	Heavy	Medium	CAT-F
EC-225	11,000	16.2	Heavy	Medium	CAT-F
CH-46E	11,022	15.24	Heavy	Medium	CAT-F
EC101-411	14,600	18.59	Heavy	Medium	CAT-F
CH-47A	14,969	18.01	Heavy	Medium	CAT-F
S-60	15,649	21.95	Heavy	Medium	CAT-E
HC6	22,980	18.29	Heavy	Medium	CAT-E
CH-53K	33,566	24.08	Heavy	Medium	CAT-E
Mi-26T	56,000	32	Heavy	Medium	CAT-D

Table 6: Example of helicopter categories based on the conventional/industry, ICAO, and RECAT-EU criteria

ID number	Helicopter	Mass (kg)	Velocity (knots)	Height (feet)
1	CH-53	11,000	90	200
2	CH-53	10,800	90	200
3	CH-53	10,600	90	200
4	CH-53	10,000	90	200
5	Puma	5,700	65	200
6	Puma	6,500	70	200
7	Puma	6,400	70	200

Table 7: Flight parameters of the CH-53 and Puma helicopters

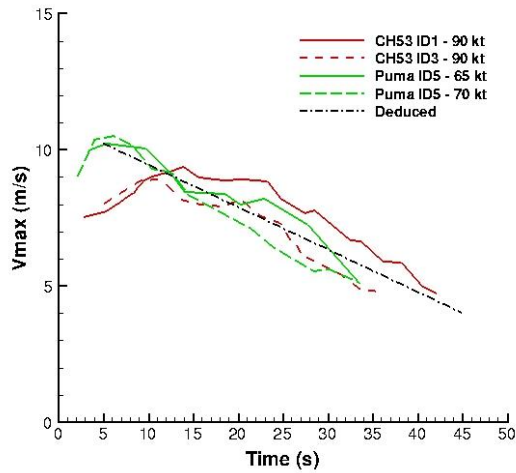


Figure 3: Measured maximum tangential velocity versus vortex age for the Sikorsky CH-53 and Puma helicopter vortices

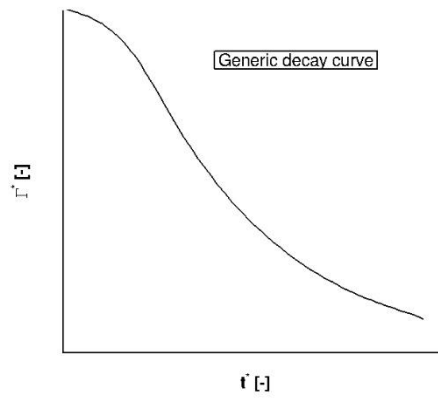


Figure 4: Generic dimensionless decay curves for various heavy aircraft

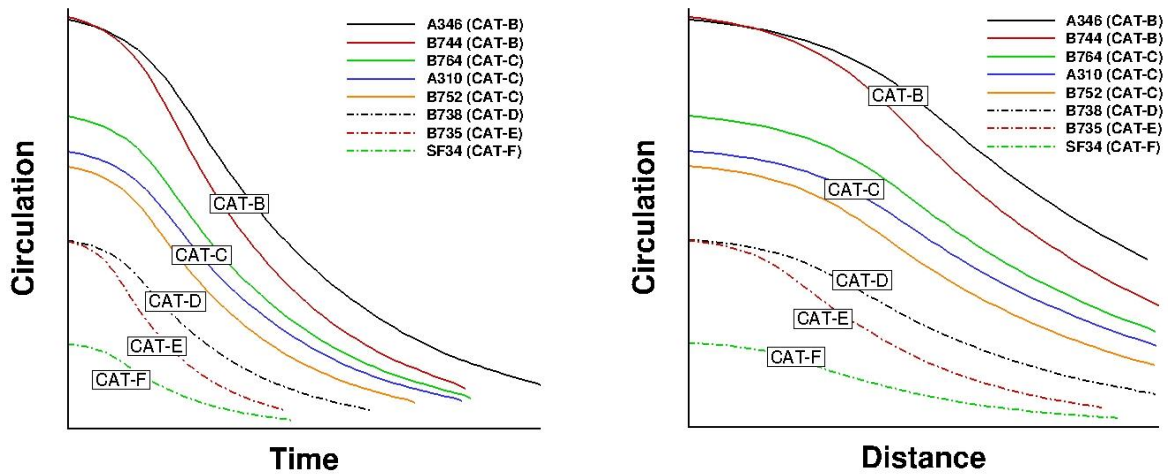


Figure 5: Dimensionless decay curves for various aircraft types as function of the time (left) and distance (right)

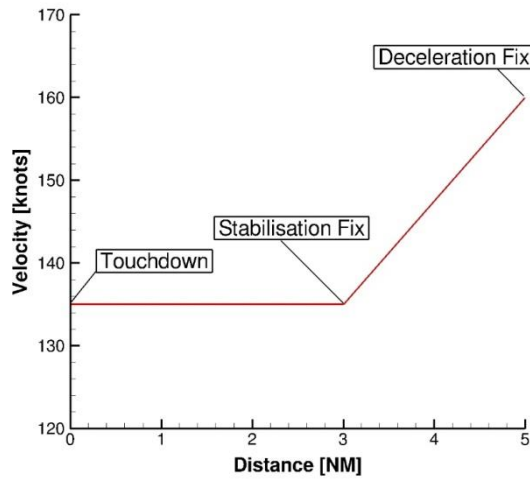


Figure 6: Generic speed profile applicable to fixed-wing aircraft on approach

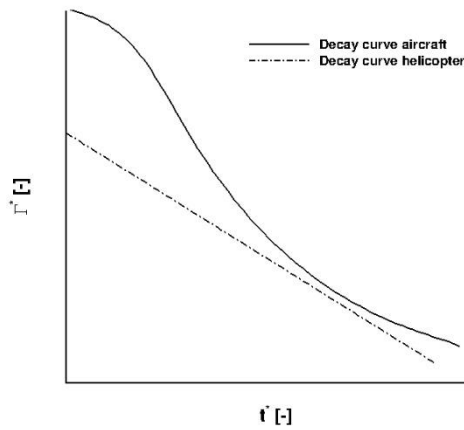


Figure 7: Comparison of the generic dimensionless decay curves for fixed-wing aircraft (solid line) and helicopter (dashed line)

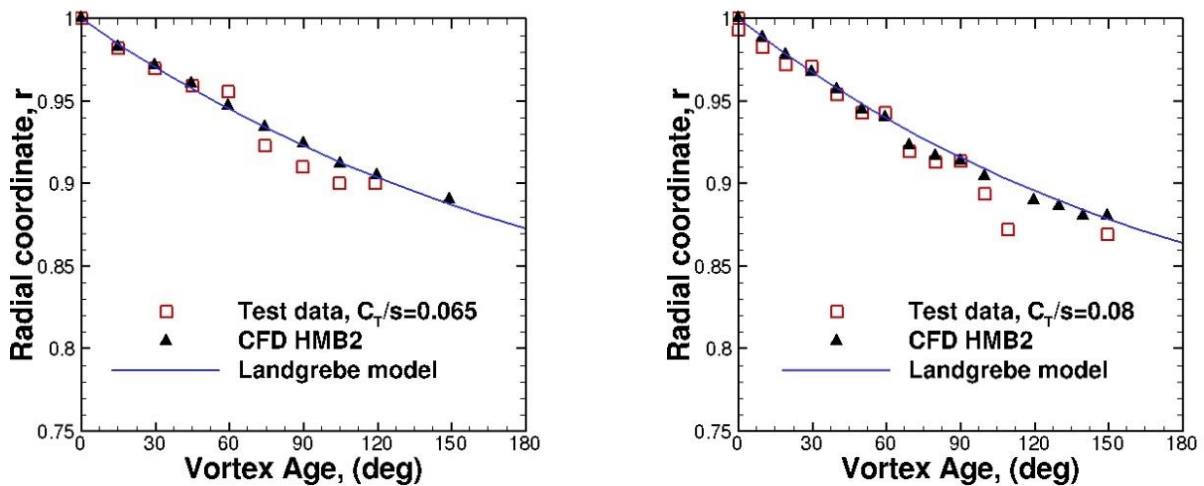


Figure 8: Comparison of the radial displacements of the tip vortices as function of the vortex age (in degrees), with the prescribed wake-model of Landgrebe [10] and experimental data of Swanson [11] for two blade loading coefficients, $C_T/\sigma=0.065$ and 0.080 . This case corresponds to the full-scale S-76 rotor with 60% taper-35° swept tip and $M_{tip}=0.605$

Glideslope	Speed	Start Height	Length of approach path
3°	70 knots	955ft	3.0 NM
6°	60 knots	2,000ft	3.1 NM
9°	40 knots	2,000ft	2.1NM
12°	40 knots	2,000ft	1.5 NM

Table 8: Glideslope, speed, height, and length of approach path for various helicopter approaches

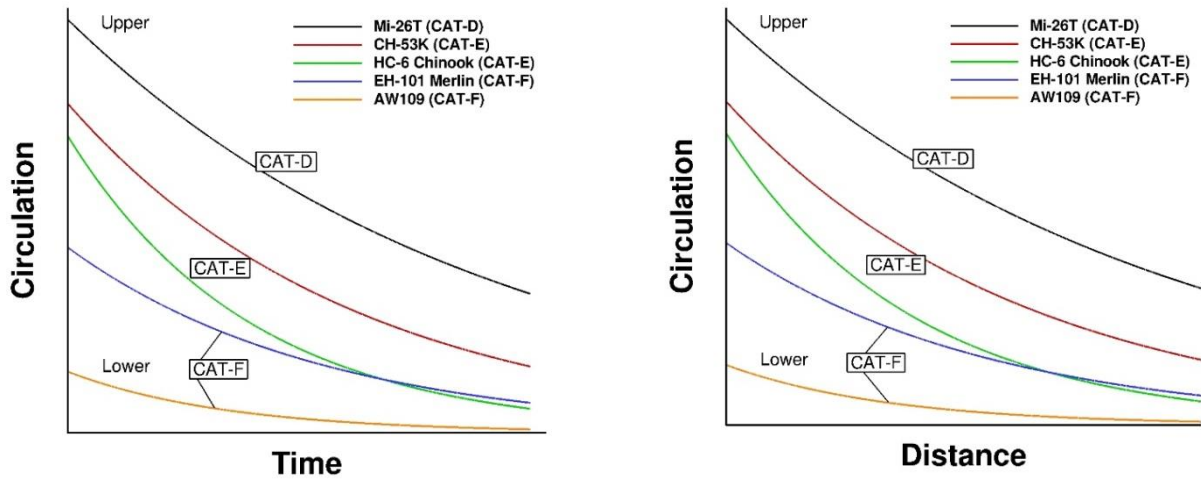


Figure 9: Dimensionless decay curves for various helicopter types as function of the time (left) and distance (right)

Variable	Description
V_T (m/s)	Velocity of the encounter vortex at time t
R (m)	Rotor radius
Ω (rad/s)	Nominal rotor speed
μ	Advance ratio
γ	Lock number
C_T	Thrust coefficient based on the MTOW
h (m)	Distance from the main rotor to CG
N_b	Number of blades
K_β	Torsional stiffness
I_{yy} (kg m ²)	Moment of inertia around the y – axis

Table 9: Physical and geometric parameters of a helicopter used for the pitch angle equation

Cases	Leader	Follower
1	Helicopter	Fixed-wing aircraft
2	Fixed-wing aircraft	Helicopter
3	Helicopter	Helicopter

Table 10: Cases considered here to suggest separation minima applicable to the pair fixed-wing aircraft/helicopter following the RECAT-EU Wake Turbulence scheme

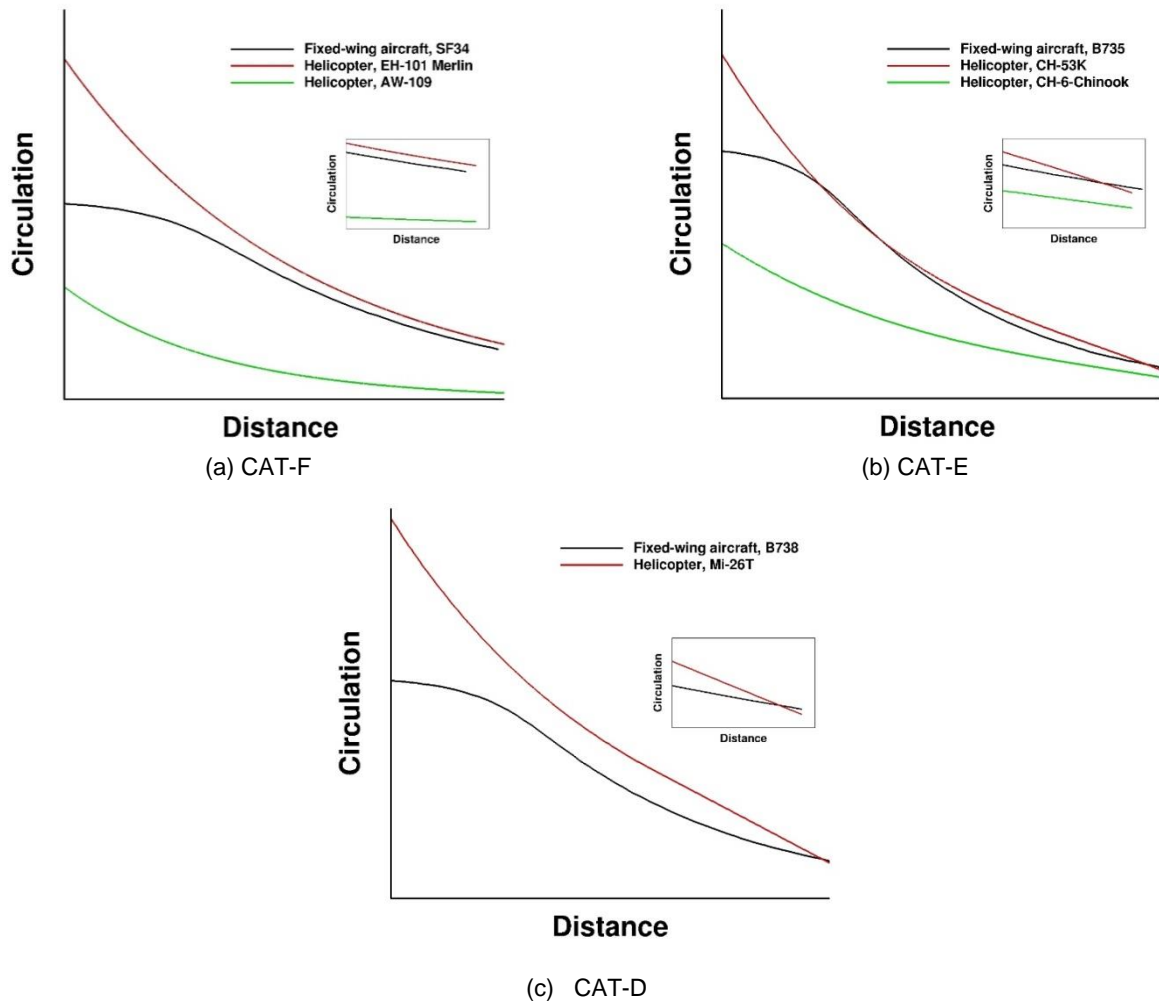


Figure 10: Comparison between fixed-wing aircraft and helicopter wake vortex circulation for CAT-F, CAT-E, and CAT-D

RECAT-EU scheme		"SUPER HEAVY"	"UPPER HEAVY"	"LOWER HEAVY"	"UPPER MEDIUM"	"LOWER MEDIUM"	"LIGHT"
Leader / Follower		"A"	"B"	"C"	"D"	"E"	"F"
"SUPER HEAVY"	"A"	N/A	N/A	N/A	N/A	N/A	N/A
"UPPER HEAVY"	"B"	N/A	N/A	N/A	N/A	N/A	N/A
"LOWER HEAVY"	"C"	N/A	N/A	N/A	N/A	N/A	N/A
"UPPER MEDIUM"	"D"						5 NM
"LOWER MEDIUM"	"E"						4 NM
"LIGHT"	"F"						3 NM

Table 11: Suggested RECAT EU WT distance-based separation minima on approach for a helicopter as a leader and a fixed-wing aircraft as a follower

Parameters	SA 330 Puma	CH-53 K	Mi-26T
Rotor radius, R	7.54 m	12.04 m	16 m
Solidity, σ	0.0917	0.1591	0.1818
MTOW	5,805 kg	33,566 kg	56,000 kg
Thrust, C_T	0.0059	0.0053	0.0028
Lock number γ	11	11	11
Blade flap stiffness, K_b	1	1	1
Number of blades, N_b	4	7	8
Distance from the main rotor to CG, h	2 m	2 m	2 m
Advance velocity, μ	0.12	0.12	0.12

Table 12: Physical characteristics of the SA 330 Puma, CH-53K, and Mi-26T helicopters

	Follower - Helicopter		
	Mi-26T (CAT-D)	CH-53K (CAT-E)	Puma (CAT-F)
Leader - FWA			
A346 (CAT-B)	1.46° (4 NM)	2.00° (5 NM)	3.23° (7 NM)
B744 (CAT-B)	1.16° (4 NM)	1.50° (5 NM)	2.20° (7 NM)
B764 (CAT-C)	1.23° (3 NM)	1.58° (4 NM)	2.25° (6 NM)
A310 (CAT-C)	1.07° (3 NM)	1.36° (4 NM)	1.92° (6 NM)
B752 (CAT-C)	0.88° (3 NM)	1.07° (4 NM)	1.38° (6 NM)
B738 (CAT-D)			1.02° (5 NM)
B735 (CAT-E)			0.74° (4 NM)
SF34 (CAT-F)			0.66° (3 NM)

Table 13: Maximum values of pitch angles when a helicopter encounters a wake generated by a fixed-wing aircraft with the distance (in bracket) based on RECAT-EU (see Table 2)

	Follower CAT-D	Follower CAT-E	Follower CAT-F
Leader CAT-D	0.92° (2.5 NM)	1.64° (2.5 NM)	0.95° (5 NM)
Leader CAT-E	0.48° (2.5 NM)	0.85° (2.5 NM)	0.68° (4 NM)
Leader CAT-F	0.22° (2.5 NM)	0.40° (2.5 NM)	0.73° (3 NM)

Table 14: Maximum values of pitch angles when a helicopter encounters a wake generated by a helicopter with the distance (in bracket) based on RECAT-EU (see Table 2)

RECAT-EU scheme		“SUPER HEAVY”	“UPPER HEAVY”	“LOWER HEAVY”	“UPPER MEDIUM”	“LOWER MEDIUM”	“LIGHT”
Leader / Follower		“A”	“B”	“C”	“D”	“E”	“F”
“SUPER HEAVY”	“A”	N/A	N/A	N/A	N/A	N/A	N/A
“UPPER HEAVY”	“B”	N/A	N/A	N/A	N/A	N/A	N/A
“LOWER HEAVY”	“C”	N/A	N/A	N/A	N/A	N/A	N/A
“UPPER MEDIUM”	“D”						5 NM
“LOWER MEDIUM”	“E”						4 NM
“LIGHT”	“F”						3 NM

Table 15: Separation minima on approach for a helicopter as a leader and a helicopter as a follower